Journal of Cleaner Production xxx (2015) 1–11

Contents lists available at ScienceDirect

Journal of Cleaner Production

journal homepage: www.elsevier.com/locate/jclepro

# Enhancement of chromium removal efficiency on adsorption and photocatalytic reduction using a bio-catalyst, titania-impregnated chitosan/xylan hybrid film

Jirapat Ananpattarachai, Puangrat Kajitvichyanukul*

*Centre of Excellence on Environmental Research and Innovation, Faculty of Engineering, Naresuan University, Thailand*

ARTICLE INFO

*Article history:*
Received 22 March 2015
Received in revised form
19 October 2015
Accepted 22 October 2015
Available online xxx

*Keywords:*
Chromium
$TiO_2$
Chitosan
Photocatalysis
Adsorption
Bio-catalyst

ABSTRACT

A novel bio-catalyst, titania-impregnated chitosan/xylan hybrid film was prepared by addition of titanium dioxide in the mixture solution of chitosan and xylan in acetic acid. The structure and surface morphology of the obtained catalyst were characterized by X-ray diffraction, and scanning electron microscope. The adsorption and photocatalytic activity of this photocatalyst were evaluated by photocatalytic reduction of chromium(VI) in aqueous solution under ultraviolet irradiation. From the rough surface modification from xylan addition and the chelating ability of chitosan, the enhancement of chromium(VI) removal by adsorption and photocatalysis of this bio-catalyst was pronounced. The photocatalytic reduction rate of chromium(VI) was $0.56 \times 10^{-3}$ and $0.03 \times 10^{-3}$ ppm-min for the titania bio-catalyst and titania nanopowder, respectively. The adsorption of chromium(VI) followed the Langmuir adsorption isotherm model. Pseudo-first order model well described the photocatalytic reduction reactions of the bio-catalyst. Significant dependence of chromium(VI) removal on the titania and chitosan loading can be explained in terms of the relationship between kinetics of chromium(VI) photocatalytic reactions and the loading amount of each chemical. According to the Langmuir–Hinshelwood model, the photocatalytic rate constant of surface reaction of chromium(VI) was increased with an increasing of chemical loading (titania and chitosan) in bio-catalyst. Results from this work exhibited that the novel titania-impregnated chitosan/xylan hybrid film can be a potential material for heavy metal removal in photocatalytic process.



## 1. Introduction

Photocatalysis is a promising technology for environmental abatement. As an efficient means for pollution treatment, this technology is widely investigated to remove organic and inorganic contaminants from water and wastewater (Said et al., 2015). Titanium dioxide has been widely used as a photocatalyst due to its activity, photostability, non-toxicity and commercial availability. There are previous studies show that Cr(VI) can undergo photocatalytic reduction and deposit on the surface of titanium dioxide (Kajitvichyanukul and Watcharenwong, 2003). However, $TiO_2$ exhibits low adsorption activity and difficulty in separating the catalyst from the effluent. The latter problem could be avoided by using the $TiO_2$ films applied on different types of substrates such as stainless steel (Kajitvichyanukul and Amornchat, 2005) and glass plate (Kajitvichyanukul et al., 2005). As a result, $TiO_2$ is widely applied in an immobilized form to treat pollutants from water or wastewater. In this recent work, the synthesis of new bio-catalyst as $TiO_2$-impregnated chitosan/xylan hybrid film was purposed with the primary objective is to enhance the adsorption ability of $TiO_2$ in photocatalytic process. Chitosan is biopolymer material produced from N-deacetylation of chitin. It has a superb ability in adsorption pollutants especial metal ions (Leceta et al., 2013). It is a powerful chelating agent, which is easy to form complexes with the combination of chitosan on $TiO_2$ film. It is expected that the adsorption ability of $TiO_2$ would be enhanced.

In the present paper, a novel bio-catalyst material employing nano$TiO_2$ impregnated chitosan/xylan film (TCF) was designed using a simple surface coating method. Both chitosan and xylan are natural nontoxic biomaterials with low cost and easy availability from biomass. Xylans polysaccharides are the group of hemicelluloses that are found in plant cell walls and some algae. They

* Corresponding author.
*E-mail address:* puangratk@nu.ac.th (P. Kajitvichyanukul).

http://dx.doi.org/10.1016/j.jclepro.2015.10.098
0959-6526/

contain predominantly β-D-xylose which are linked by β-1,4-glycosidic bonds and branched by α-1,2-glycosidic bonds with 4-O-methylglucosidic acid groups (Dodd et al., 2011). Recently, the hybrid materials from the complexing of chitosan with xylan have shown ability to form selective stable complex with heavy metals (Dai et al., 2012). The increasing of highly porous structure in hydrogel of nano$TiO_2$ complexing with chitosan and xylan was introduced by Wu et al. (2014). With the modification of the $TiO_2$ catalyst on the chitosan/xylan hybrid film, the performance in the photocatalytic reaction could be greatly enhanced. However, there are few reports that focused on application of this bio-catalyst in pollutant removal.

In this work, we investigated the application of TCF bio-catalyst for Cr(VI) removal by both adsorption and photocatalysis. Cr(VI) is a toxic heavy metal widely used in many industries and always found in wastewater stream. The risk and hazard of this heavy metal is discussed widely in the previous work (Eastmond et al., 2008). Cr(VI) was selected to be the tested pollutant in this work. The effects of pH, contact time and initial concentration on the adsorption capacities of Cr(VI) on this material were reported. The equilibrium adsorption isotherms of Cr(VI) onto the bio-catalyst were determined by the Langmuir and Freundlich equations. The photocatalytic activity was evaluated by the decrease of Cr(IV) concentration after irradiation. Effects of $TiO_2$ and chitosan loadings in TCF materials on photocatalytic activity were investigated. The kinetics of photocatalytic reduction of Cr(VI) were also investigated in this work. The results from this work would be useful for the application of the novel organic–inorganic bio-catalyst concerning the heavy metal removal with enhanced adsorption and photocatalytic ability.

## 2. Materials and methods

### 2.1. Chemicals and reagents

Xylan, titanium (IV) oxide nanopowder (Degussa P25, <25 nm particle size, 99.7% trace metals basis), and chitosan flake with a molecular weight of 600,000 g/mol were purchased from Sigma–Aldrich, Singapore. The other chemicals used were of analytical grade obtained from Merck, Thailand. All aqueous solutions were prepared using purified water with a resistance of 18.2 MΩ cm.

### 2.2. Preparation of nano$TiO_2$ impregnated chitosan/xylan hybrid films (TCF)

The procedure for the preparation of nano$TiO_2$ impregnated chitosan/xylan hybrid films (TCF) was prepared. First, 1.5% w/w chitosan flake was dissolved in a 50 mL of the $CH_3COOH$. Then, 0.1% w/w xylan and 0.4% w/w of nano$TiO_2$ powder were added to the solution and stirred for 8 h with ultrasonic treatment for 15 min at half hour intervals. Subsequently, another 50 mL of 0.1 M $CH_3COOH$ was added. The slurry was stirred continuously for 24 h to obtain the final transparent viscous solution. After this typical procedure, the amounts of nano$TiO_2$ (0.2, 0.4, 0.6, and 0.8% w/w) and chitosan flake (1, 1.5, 2 and 2.5% w/w) were varied to obtain different properties of TCF film.

The pieces of 50 mm × 60 mm × 2 mm glass plates were used as support to immobilize the prepared TCF catalyst. The glass plates were cleaned thoroughly and dried before use. Then, the viscous solution was spread on the glass plate and placed to dry at 100 °C inside an oven for 7 h alternately after deposition. The chitosan–xylan hybrid film (CF) was prepared as a control using the same method without the addition of nano$TiO_2$. Both $TiO_2$, CF, and CTF were used further in adsorption and photocatalysis experimental parts.

### 2.3. Characterization of nano$TiO_2$ impregnated chitosan/xylan hybrid films (TCF)

Surface morphology of the TCF, CF, and $TiO_2$ powder was studied by scanning electron microscope (SEM), a field emission Hitachi S-4500 SEM operated at 15 kV. This SEM is equipped with energy dispersive X-ray spectroscopy (EDS) to examine the elemental composition in the investigated samples. Small pieces of the prepared photocatalyst were peeled off from the glass plate and stuck on stubs using double-sided tape. Before the samples were analysed, they were sputtered with a layer of gold film to prevent the occurrence of charging effect. Whereas, the phase composition of the prepared photocatalyst was studied using the powder and plate XRD technique. The patterns were recorded on a Shimadzu X-ray Diffractometer (XRD-6000) using Cu Kα radiation. Diffraction patterns were taken over the 2θ range 5–60°.

### 2.4. Adsorption and photocatalysis experiments

For Cr(VI) removal by adsorption and photocatalysis process, the solution was prepared by dissolving potassium dichromate ($K_2Cr_2O_7$) in distilled water. In the adsorption process, five pieces of TCF were placed in the chromium solution. The Cr(VI) solutions were equilibrated in the dark. The samples were taken during the time interval for Cr(VI) analysis to obtain the effect of pH and adsorption isotherm. The adsorption capacity of each adsorption experiment was calculated as the amount adsorbed Cr(VI) on the surface of TCF per gram of TCF used.

For photocatalytic process, prior to irradiation, the TCF was placed in a solution in 1000 mL of photocatalytic reactor. The solution was illuminated by a 10 W germicide lamp with a nominal wavelength range of 254 nm located at the centre of the reactor. Air was bubbled through the reaction solution to ensure a constant supply of nitrogen gas and to give agitation effect to achieve an equilibrium state of Cr(VI) and TCF. The dark adsorption was conducted until it reached equilibrium and, then, a lamp was turned on to illuminate the TCF for 180 min. The Cr(VI) solution was agitated thoroughly by the magnetic stirrer. The 1.0 mL of the sample after illumination was syringed out for Cr(VI) analysis using a 1.5-diphenylcarbazide (BDH) colorimetric method (Zhou et al., 1993). The Cr(VI) determination was measured at the absorbance at 540 nm in acid solution with a PerkinElmer Lambda 20 UV–vis spectrometer. The residual Cr(VI) concentration in the aqueous solution was plotted as a function of time. The observed rate constant ($k_{obs}$) from each experimental condition was calculated. All experiments in the adsorption and photocatalytic reactions were duplicated.

## 3. Results and discussion

### 3.1. Material characterization of TCF bio-catalyst

Molecular structures of chitosan and xylan are shown in Fig. 1. Both chemicals are biomaterials that are widely available in nature. Chitosan (Fig. 1a) has an amino group in its structure. Xylan (Fig. 1b) contains predominantly β-D-xylose units. Both chemicals presented their unique characteristics in CF and TCF as detected by XRD pattern in Fig. 2. Nano$TiO_2$ crystalline (Fig. 2a) was mainly composed of anatase phase (as shown by the main peak of 2θ at 25.3°) and rutile phase (2θ at 27.5°). Normally, chitin–chitosan was outstanding demonstrated peak of 2θ in two positions at 9 and 21° (Sankararamakrishnan et al., 2005). However, the broad peak at approximately 21° also indicates some short-range order in the amorphous polymeric structure of the hemicellulose in xylan (Cara et al., 2013). In our work, two peaks at 9 and 21° in XRD spectra

Please cite this article in press as: Ananpattarachai, J., Kajitvichyanukul, P., Enhancement of chromium removal efficiency on adsorption and photocatalytic reduction using a bio-catalyst, titania-impregnated chitosan/xylan hybrid film, Journal of Cleaner Production (2015), http://dx.doi.org/10.1016/j.jclepro.2015.10.098

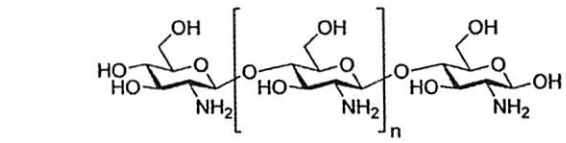

a) chitosan

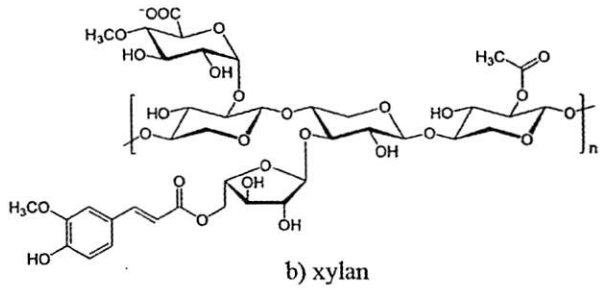

b) xylan

**Fig. 1.** Molecular structures of (a) chitosan and (b) xylan.

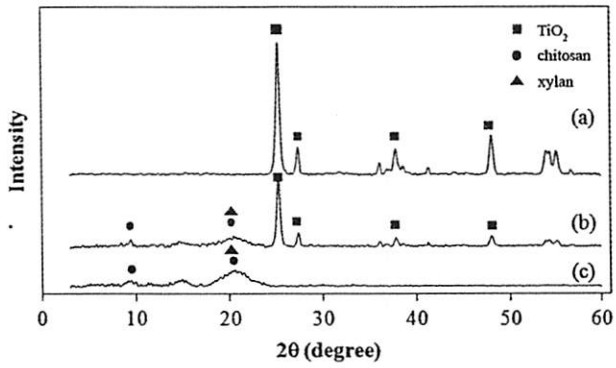


**Fig. 2.** X-ray diffraction patterns of (a) $TiO_2$ powder (b) TCF (1.5% w/w chitosan, 0.4% w/w of $TiO_2$, and 0.1% w/w xylan), and (c) CF (1.5% w/w chitosan and 0.1% w/w xylan).

were pronounced in both CF and TCF materials demonstrated the composition of both chemicals in the hybrid film. In addition, many peaks of $TiO_2$ with anatase and rutile phases also clearly observed in TCF spectrum. These results could be confirmed that $TiO_2$ can be successfully impregnated into the chitosan/xylan hybrid film and the employed synthesis method did not cause any change in identity of chitosan, xylan, and $TiO_2$ (Fig. 2).

The SEM images of $TiO_2$ powder, CF and TCF are shown in Fig. 3. Fig. 3a reveals the uniform size of $TiO_2$ crystalline. Fig. 3b displays the morphology of chitosan/hybrid film (with 1.5% w/w of chitosan and 0.1% w/w xylan). The rough surface film was clearly seen. The insert picture exhibits the well blend of the xylan hemicellulose and the viscous chitosan. Fig. 3c reveals the morphology of TCF film with 1.5% w/w of chitosan. This picture indicates the intrusion of $TiO_2$ powder in the chitosan/xylan hybrid film. The $TiO_2$ nanoparticles were well dispersed on the TCF film. However, the application of the high amount of chitosan (for example, 2.5% w/w of chitosan) in chitosan/xylan solution in film preparation process initiated high viscosity of the mixture solution. The morphology of the TCF with the high chitosan loading was shown in Fig. 3d. Apparently, the dense film of chitosan/xylan hybrid material shielded the nano$TiO_2$ powder. The different morphologies of the TCF from the preparation conditions exert effect on the photocatalytic activity discussed in the following section. The EDS spectrum of the TCF, 0.4% w/w $TiO_2$ with 1.5% w/w of chitosan and 0.1% w/w xylan is shown in Fig. 3e. The Ti peaks are pronounced in the TCF material. From overall characterization of the TCF, the existence of $TiO_2$ crystalline impregnated on the chitosan/xylan is clearly illustrated.

### 3.2. Role of pH on TCF bio-catalyst surface

Zeta potential ($pH_{pzc}$) of TCF bio-catalyst was measured to obtain the surface property. The significance of $pH_{pzc}$ of the photocatalyst on pollutant removal has been discussed in many previous works (Chong et al., 2015). In this work, the $pH_{pzc}$ of TCF is 6.2. In addition, the $pK_a$ of chitosan ranges from 6.3 to 7.2 (Gerente et al., 2007), depending on factors including the degree of acetylation and ionic strength (Crini and Badot, 2008). The protonated amino group ($-NH_3^+$) on the sorbent in a TCF structure tentatively plays a significant role in decreasing of $pH_{pzc}$ of TCF into a positive region. The adsorption of Cr(VI) onto TCF surface across a pH range was followed electrostatic interaction between the sorbent–sorbate systems as represents by the Cr(VI) adsorption efficiency in Table 1. Charges of TCF and Cr(VI) are also represented in the same table.

The highest adsorption of TCF is occurred in acidic solution at pH 3. This could be explained that at low pH (acidic solution), most of the functional groups such as $-NH_3$, $-OH$ and $-CH{=}N-$ in the TCF were protonated and presented in the positively charged form, while the Cr(VI) existed in the form of $HCrO_4^-$ or $Cr_2O_7^{2-}$. The mechanism of the adsorption process of Cr(VI) on TCF in acidic pH are likely to be the ionic interactions of the negative charge of Cr(VI) with the amino groups of the chitosan. In aqueous solution at pH 3, Cr(VI) exists in the form of $HCrO_4^-$ and the amino groups of chitosan ($R-NH_2$) became protonated.

$$R-NH_2 + H^+ \leftrightarrow R-NH_3^+ \quad (1)$$

This protonated amino group ($-NH_3^+$) proceed due to the electrostatic interaction between these two oppositely charged ions.

$$R-NH_3^+ + HCrO_4^- \leftrightarrow R-NH_3 \ldots . HCrO_4^- \quad (2)$$

The attraction force between a positive charge of TCF surface and the negative charge of Cr(VI) is predominance in this pH region.

In basic pH, the amino groups on the TCF are not fully protonated due to insufficient $H^+$ concentration. In addition, the surface of TCF is dominated by $OH^-$ that is the same charge with $CrO_4^{2-}$ of Cr(VI) species in aqueous solution. As a result, the repulsion of negative species from both TCF and Cr(VI) is dominated and prevented the adsorption process. Thus, much lower amount of Cr(VI) being adsorbed on the TCF surface in basic pH solution. In addition, the quantity of adsorption capacity also decreased with an increase of pH, owing to the interaction between $OH^-$ and metal ions to form hydroxide precipitate. This behaviour was also seen in the application of chitosan nanoparticles that had been used in the adsorption of acid dyes (Cheung et al., 2009). Results from this work are also in good agreement with the recent work of porous chitosan–xylan–$TiO_2$ hybrid that provided a highly efficient sorption capability of heavy metals (Wu et al., 2014). The aqueous pH played an important role on the surface of the hybrid film for both CF and TCF and was the controlled parameter for the adsorption process.

### 3.3. Adsorption of Cr(VI) by TCF, CF, and $TiO_2$

The comparison between the adsorption of Cr(VI) on TCF, CF, and $TiO_2$ at pH 3 is shown in Table 2. The removal percentages of Cr(VI) by adsorption process were 53.22, 31.06, and 0.84% and the adsorption capacity of Cr(VI) are 351.82, 230.78, and 28.72 mg/g for

Please cite this article in press as: Ananpattarachai, J., Kajitvichyanukul, P., Enhancement of chromium removal efficiency on adsorption and photocatalytic reduction using a bio-catalyst, titania-impregnated chitosan/xylan hybrid film, Journal of Cleaner Production (2015), http://dx.doi.org/10.1016/j.jclepro.2015.10.098

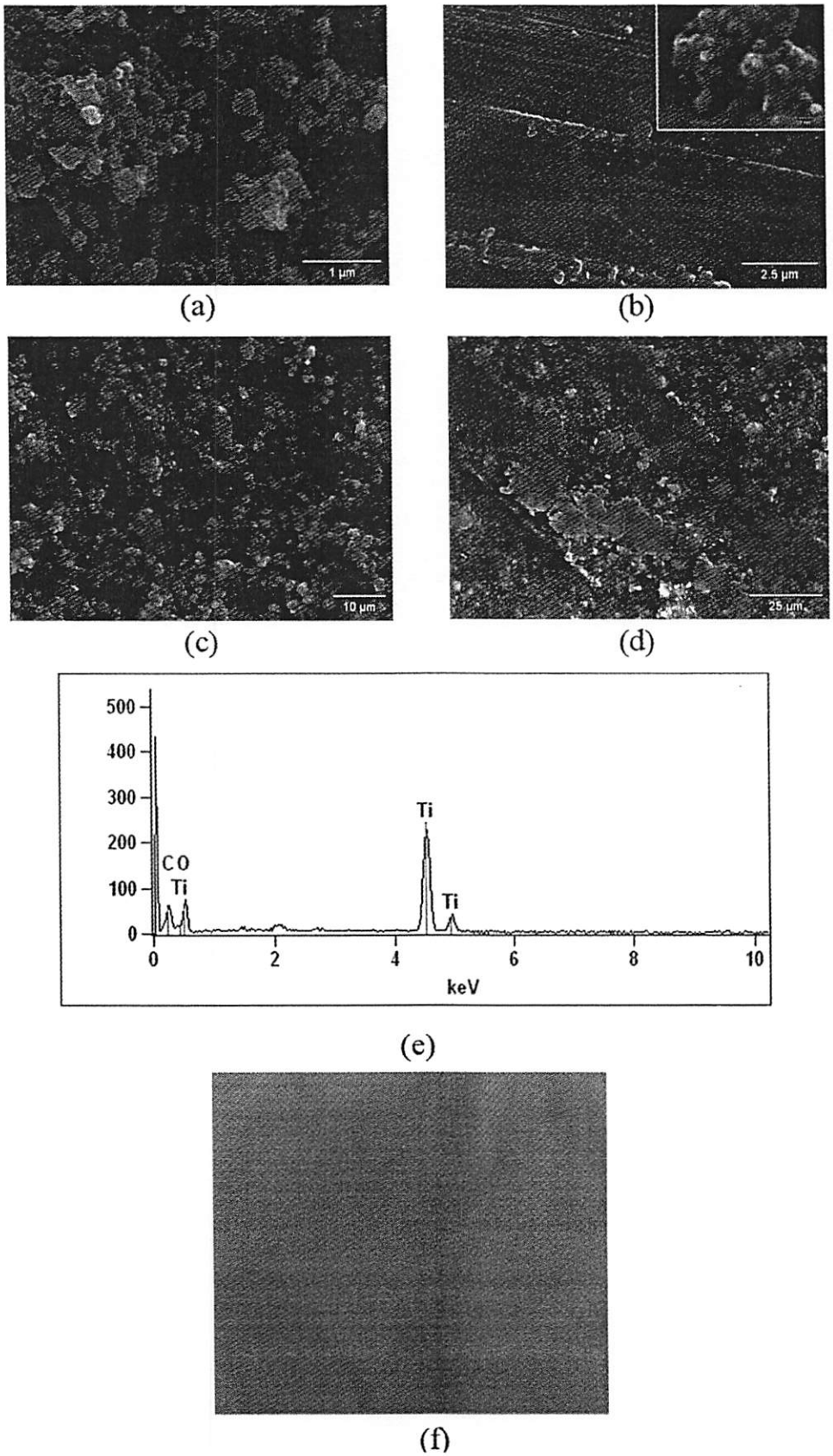


**Fig. 3.** SEM images of (a) $TiO_2$ nanoparticles, (b) CF (1.5% w/w chitosan and 0.1% w/v xylan), (c) TCF (1.5% w/w chitosan, 0.4% w/w $TiO_2$, and 0.1% w/w xylan), (d) TCF (2.5% w/w of chitosan, 0.4% w/w $TiO_2$ and 0.1% w/w xylan), (e) EDS spectrum of TCF (1.5% w/w chitosan, 0.4% w/w $TiO_2$, and 0.1% w/v xylan), and (f) a photograph of titania-impregnated chitosan/xylan hybrid film.

Please cite this article in press as: Ananpattarachai, J., Kajitvichyanukul, P., Enhancement of chromium removal efficiency on adsorption and photocatalytic reduction using a bio-catalyst, titania-impregnated chitosan/xylan hybrid film, Journal of Cleaner Production (2015), http://dx.doi.org/10.1016/j.jclepro.2015.10.098

**Table 1**
Percentage of Cr(VI) removal by adsorption onto TCF surface at different pH.

| pH | % of Cr(VI) removal | TCF species | Cr(VI) species |
|---|---|---|---|
| 3 | 53.22 | (TCF)-$NH_3^+$ | $HCrO_4^-$ |
| 5 | 35.23 | (TCF)-$NH_3^+$ | $HCrO_4^-$ or $Cr_2O_7^{2-}$ |
| 7 | 12.3 | (TCF)-$OH^-$ | $CrO_4^{2-}$ |
| 9 | 10.2 | (TCF)-$OH^-$ | $CrO_4^{2-}$ |
| 11 | 8.3 | (TCF)-$OH^-$ | $CrO_4^{2-}$ |
| 12 | 4.2 | (TCF)-$OH^-$ | $CrO_4^{2-}$ |

TCF, CF, and $TiO_2$, respectively. Results showed that $TiO_2$ powder provided the lowest Cr(VI) removal percentage among three materials. The adsorption ability of chitosan in both CF and TCF plays an important role in this process. In comparison of Cr(VI) adsorption ability between TCF and CF, Cr(VI) adsorbed slightly better on TCF than on CF. This result can be ascribed to the presence of xylan and $TiO_2$ in the TCF. The impregnation of $TiO_2$ on the surface of CF increased the roughness of the film as seen from the SEM morphology in Fig. 3. It is also reported that the complexing of nano$TiO_2$ with chitosan and xylan introduced highly porous surface of the material and enhanced high adsorption ability of heavy metals (Wu et al., 2014). As the increasing number of active sites accessible for Cr(VI) anions due to the complexing of $TiO_2$ with chitosan and xylan was increased, the adsorption of Cr(VI) on this film was enhanced.

The UV–vis spectrograph of the Cr(VI) with 1 ppb detection limit is shown in Fig. 4a. Adsorption of Cr(VI) on the TCF with different initial Cr(VI) concentration is shown in Fig. 4b and c. Amount of adsorbed Cr(VI) was increased with time and attained equilibrium within 120 min which is the equilibration time required for maximum Cr(VI) adsorption on TCF surface. The adsorption amount of Cr(VI) had an increasing growth from 280 mg/g to 540 mg/g as the initial Cr(VI) concentration increased from 20 ppm to 300 ppm. However, the removal percentage decreased with increasing initial Cr(VI) concentration. The removal percentage of Cr(VI) slowly decreased when initial Cr(VI) concentration was higher than 200 ppm. When further Cr(VI) concentration is increasing, the removal percentage rapidly decreased. A possible reason is that the adsorption sites on the TCF were not fully occupied at a low Cr(VI) concentration, thereby the adsorption amount of Cr(VI) and the removal percentage increased. When the concentration of Cr(VI) in solution was increase, the number of Cr(VI) molecule was beyond the adsorption capacity of the adsorbent. Consequently, the decreasing trend of Cr(VI) removal became minimal.

Two adsorption isotherms models, Langmuir and Freundlich, were applied as presented in Fig. 4d and e. In Langmuir isotherm, $Q_0$ is maximum adsorption at monolayer coverage, mg/g, and $b$ is Langmuir constant related to the affinity of binding sites, L/mg and it is a measure of energy of adsorption. The Langmuir equation was shown below:

$$C_e/(x/m) = 1/(Q_0 b) + C_e/Q_0 \quad (3)$$

where $C_e$ is the equilibrium concentration of Cr(VI), ppm, $x/m$ or $q_e$ is amount of adsorbed Cr(VI) at equilibrium per unit mass of TCF, mg/g. The linear plot of $C_e/(x/m)$ vs. $C_e$ in Fig. 4c shows that the adsorption of Cr(VI) onto TCF surface obeys Langmuir adsorption isotherm with the values of $Q_0$ as of 500 mg/g and $b$ as of 0.075 L/mg. The correlation coefficient of linear regression for Langmuir isotherm is 0.9931.

Freundlich equation was also used to adsorption of Cr(VI) onto TCF surface. The Freundlich characteristic constants, $k_f$ and $n$, are the indicators of the adsorption and the adsorption intensity, respectively. The Freundlich isotherm is represented by the equation.

$$\log (x/m) = (1/n) \log C_e + \log k_f \quad (4)$$

where $C_e$ is the equilibrium concentration of Cr(VI), ppm, $x/m$ is the amount of adsorbed Cr(VI) at equilibrium per unit mass of $TiO_2$/chitosan film, mg/g. The plot of log $(x/m)$ versus log $C_e$ based on the above equation the same experimental results is shown in Fig. 4c with the values of $k_f$ as of 2.426 $(\text{mmol/kg})^{1-1/n}$ and $1/n$ as of 1.003. The correlation coefficient of linear regression for Freundlich isotherm is 0.7748. In comparison, the correlation coefficient for linear regression of Langmuir plot is higher than that of Freundlich plot. The value of the correlation coefficient of Cr(VI) adsorption indicates that the adsorption behaviour of Cr(VI) onto TCF tends to be a monolayer adsorption as described by Langmuir isotherm rather than Freundlich isotherm. The adsorption capacity of this TCF according to Langmuir isotherm is 564 mg/g.

Table 3 lists the comparison of the adsorption capacity of TCF with that of nanoparticles previously investigated. It can be seen that the adsorption capacity of TCF was not less than that of activated carbon, chitosan, and other adsorbent nanomaterials. This suggested that the TCF adsorbent we prepared can be considered as a promising adsorbent for Cr(VI) removal from wastewater.

### 3.4. Photocatalytic activity and kinetics of Cr(VI) removal using $TiO_2$ and TCF

To compare photocatalytic activity of $TiO_2$ and TCF, two photocatalyst experiments involving $TiO_2$ powder and TCF were applied for the photocatalytic reduction of 100 ppm Cr(VI) solution. Fig. 5 shows plot of the change in concentration of Cr(VI) in term of $C/C_0$ as a function of irradiation time ($C_0$ and $C$ are the concentrations of Cr(VI) at time zero and time $t$, respectively). The result reveals that the behaviour of photocatalytic reduction of Cr(VI) by synthesized TCF in term of kinetic study is well explained by the pseudo first order kinetics with respect to the Cr(VI) concentration (5):

$$\ln (C/C_0) = -k_{obs} \cdot t \quad (5)$$

where $k_{obs}$ is the apparent reaction rate constant, $n$ is the order of the reaction, $t$ is the reaction time. Values of $k_{obs}$ were determined from the slope of a graph which was a plot between $-\ln (C/C_0)$ and reaction time, $t$. The value $R^2$ for linear regression was calculated to exhibit the tendency of the reaction pattern to be described as pseudo-first order. From Fig. 5, results show that TCF catalyst can

**Table 2**
Percentage removal of 100 ppm Cr(VI) by adsorption using $TiO_2$, TCF, and CF.

| Material | Component | Cr(VI) (ppm) | mg of Cr(VI)/g of adsorbent | % Removal |
|---|---|---|---|---|
| TCF | 1.5% w/w chitosan, 0.1% w/w xylan and 0.4% w/w Ti | 100 | 351.82 | 53.22 |
| CF | 1.5% w/w chitosan and 0.1% w/w xylan | 100 | 230.70 | 31.06 |
| $TiO_2$ | 0.4% w/w Ti | 100 | 28.72 | 0.84 |

Please cite this article in press as: Ananpattarachai, J., Kajitvichyanukul, P., Enhancement of chromium removal efficiency on adsorption and photocatalytic reduction using a bio-catalyst, titania-impregnated chitosan/xylan hybrid film, Journal of Cleaner Production (2015), http://dx.doi.org/10.1016/j.jclepro.2015.10.098

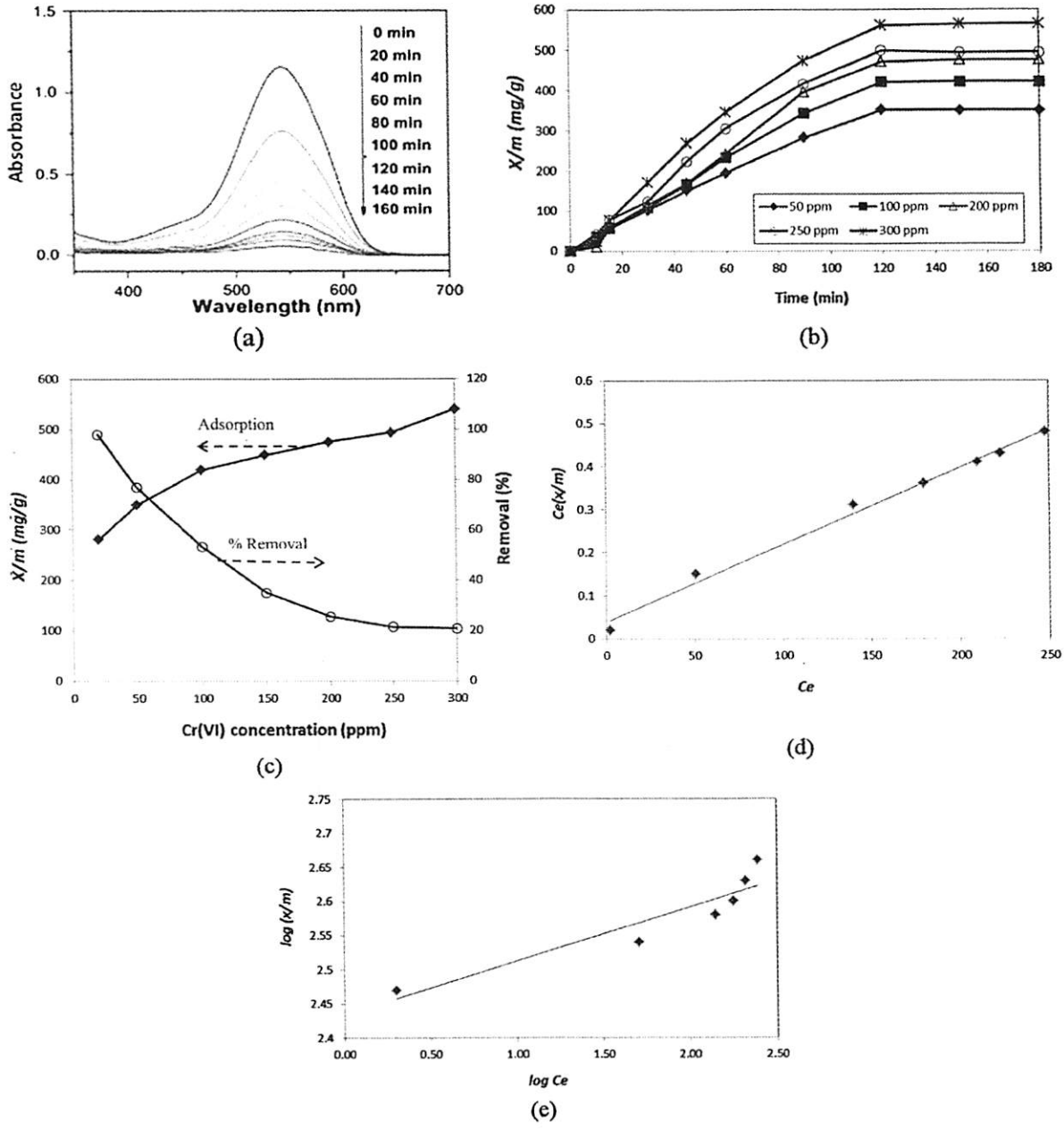


**Fig. 4.** (a) UV–vis spectrograph of the Cr(VI) with 1 ppb detection limit (b) adsorption of Cr(VI) on the TCF versus time, (c) plot of adsorbed Cr(VI) equilibrium concentration versus Cr(VI) adsorbed on TCF surface, (d) Langmuir adsorption isotherm of TCF, and (e) Freundlich adsorption isotherm of TCF. Conditions: [C] = 50–300 ppm and pH 3.

remove Cr(VI) from aqueous solution with a higher efficiency than $TiO_2$ powder. The photocatalytic reduction rate of Cr(VI) was $0.56 \times 10^{-2}$ and $0.03 \times 10^{-2}$ ppm-min for TCF and $TiO_2$ powder, respectively. Values of $k_{obs}$ from pseudo-first order equation were $0.74 \times 10^{-2}$ and $0.03 \times 10^{-2}$ $min^{-1}$ for TCF and $TiO_2$ powder respectively. This pattern suggests that the photocatalytic performance can be enhanced by the impregnation of $TiO_2$ into chitosan/xylan hybrid matrix. The Cr(VI) photocatalytic activity of the TCF was tremendously higher than that of the $TiO_2$ powder. This increasing of Cr(VI) removal performance may have been attributable to the high adsorption ability of Cr(VI) on TCF surface where plenty of $TiO_2$ is promptly reacted with Cr(VI). As discussed previously, the attraction of Cr(VI) onto the protonated amino group of chitosan (Cheung et al., 2009) and the rough morphology of TCF with high surface area from the enhancement of xylan (Wu et al., 2014) may probably the principal reasons for the high performance of this bio-catalyst.

### 3.5. Effect of chitosan loading in TCF on photocatalytic activity and kinetics

Fig. 6a Presents the effect of chitosan loading in TCF on the removal of Cr(VI) with 150 ppm initial concentration at pH 3. The amount of $TiO_2$ in all TCF materials was fixed at 0.2% w/w and the amount of chitosan was varied as of 1.0, 1.5, 2.0, and 2.5% w/w. Normally, the photocatalytic process had two stages. The Cr(VI) can be adsorbed on the surface of TCF in the dark during 30 min adsorption process in the first stage. The reduction of Cr(VI) can

Please cite this article in press as: Ananpattarachai, J., Kajitvichyanukul, P., Enhancement of chromium removal efficiency on adsorption and photocatalytic reduction using a bio-catalyst, titania-impregnated chitosan/xylan hybrid film, Journal of Cleaner Production (2015), http://dx.doi.org/10.1016/j.jclepro.2015.10.098

**Table 3**
Comparison of the adsorption properties of different absorbents for Cr(VI).

| Adsorbents | pH | $Q_{max}$ (mg/g) | References |
|---|---|---|---|
| TCF (this work) | 3 | 564 | |
| *R. communis-based activated carbon* | 7 | 200 | Makeswari and Santhi (in press) |
| *Wood apple shell-based activated carbon* | 1.8 | 151.5 | Doke and Khan (in press) |
| Cross-linked magnetic chitosan beads | 4 | 69.4 | Huang et al. (2009) |
| Modified magnetic chitosan chelating resin | 2 | 58.5 | Abou El-Reash et al. (2011) |
| Polypyrrole/$Fe_3O_4$ magnetic nanocomposite | 2 | 169.4 | Bhaumik et al. (2011) |

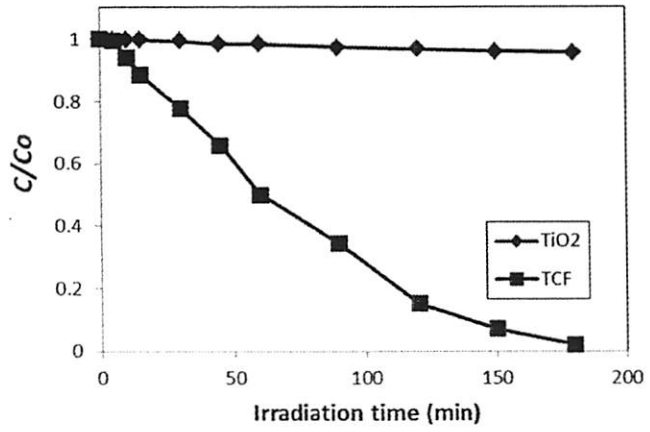


**Fig. 5.** Removal of Cr(VI) using $TiO_2$ powder and TCF in photocatalysis. Conditions: [C] = 100 ppm and pH 3.

occur by the photoreaction of Cr(VI) on TCF surface during 180 irradiation process in the second stage. Overall percentages of photocatalytic reduction of Cr(VI) is accounted for the total percentage of Cr(VI) removal. The Cr(VI) removals during dark adsorption, irradiation, and total removal percentage under variation of the amount of chitosan were shown in this graph. It was observed that the adsorption amount of Cr(VI) increased with increasing amount of chitosan. However, the Cr(VI) removal percentage during irradiation was slightly different in each condition (49.88% in average). The enhancement of the photocatalytic efficiency due to the effect of chitosan had been exploited by previous work (Nawi et al., 2011). However, its influence was clearly demonstrated in the TCF from this work. The maximum protonated amino group ($-NH_3^+$) which was a functional of the chitosan was obtained in a higher content of chitosan in TCF, and it enhanced in adsorbing Cr(VI) onto TCF surface. The photocatalytic reaction was confined mostly to adsorption capacity of media under illumination. The enhancement of photocatalytic activity was mainly attributed to the synergistic effect of the combined photocatalysis and adsorption processes.

The photocatalytic reduction of Cr(VI) using TCF with a different amount of chitosan during irradiation as a function of time is shown in Fig. 6b. Results show that within 180 min of ultraviolet light irradiation in the presence of TCF catalyst. The photocatalytic reduction of Cr(VI) using TCF can be well explained by a pseudo-first-order pattern. The values of photocatalytic reduction rate, $r$, and kinetic constant, $k_{obs}$, were calculated from the pseudo-first-order equations (Eq. (5)) and the and the half-life of Cr(VI), $t_{1/2}$, was determined from

$$C_0/C = 0.5;\ t_{1/2} = 0.693/k_{app} \quad (6)$$

Half-life, $t_{1/2}$ is a suitable indication of the rate of a first order chemical reaction of substances. It describes the time taken for the concentration of a reactant to fall to half of its initial value. Fig. 6c shows the plots of photocatalytic reduction rate, $r$, and the half-life of Cr(VI), $t_{1/2}$, as a function of the amount of chitosan. Results show that with the increase in the amount of chitosan, the reaction rate increased and the half-life of Cr(VI) decreased. It is observed that the half-life of Cr(VI) had time lessening from 101.93 min to 66.01 min as increasing amount of chitosan in TCF from 1.0% w/w chitosan to 2.0% w/w chitosan. For comparison, the reaction rate of Cr(VI) using $TiO_2$ powder (without chitosan) in the same experimental condition was $0.03 \times 10^{-2}$ ppm-min. Thus, the reaction rate enhancement of TCF with 1.0% w/w chitosan (the smallest amount of chitosan applied in TCF) was tremendously higher than that of $TiO_2$ powder by a factor of fifteen. The increasing of chitosan in TCF also exerts the apparent influence on the kinetics of photocatalytic reduction of Cr(VI). The reaction rate of TCF with 2.5% w/w chitosan was twofold higher than that of the TCF with 1.0% w/w chitosan. The rate constant of the TCF with 1.0% w/w chitosan was only $6.8 \times 10^{-3}$ $min^{-1}$, whereas the rate constant of the TCF with 2.5% w/w chitosan was $10.5 \times 10^{-3}$ $min^{-1}$. This increasing of the photocatalytic activity and kinetic was apparently derived from the influence of chitosan addition in TCF as discussed previously. Overall kinetic parameters based on the photocatalytic reduction of Cr(VI) using TCF under different amount of chitosan were also presented in Table 4. The photocatalytic reaction in the influence of chitosan amount in TCF was confined mostly to adsorption capacity of media under illumination.

### 3.6. *Effect of $TiO_2$ loading in TCF on photocatalytic activity and kinetics*

The influence of amount of $TiO_2$ loading in TCF on photocatalytic reduction of Cr(VI) with 150 ppm initial concentration and kinetics was investigated using different loading of $TiO_2$ in TCF ranging from 0.2 to 0.8% w/w. The amount of chitosan in all TCF materials was 1.5% w/w and the experiments were conducted at pH 3. The Cr(VI) removals during dark adsorption, irradiation, and total removal percentage under variation of the $TiO_2$ amount were shown in Fig. 7a. It was observed that the amount of $TiO_2$ exerts minimal influence on the Cr(VI) removal in the dark adsorption. The removal percentage of Cr(VI) during adsorption was in the range of 30.56–35.41% with 32.55% in average. However, the increasing of $TiO_2$ portion in TCF did effect on the Cr(VI) removal during the irradiation process. The overall Cr(VI) removal in photocatalysis represents a linear growth as a function of $TiO_2$ loading. The enhancement of the photocatalytic efficiency during irradiation is because the increase in the number of $TiO_2$ leads to the increase of the number of photons absorbed and, consequently, the number of Cr(VI) molecule adsorbed on the TCF surface readily reacted with the pollutants. As $TiO_2$ has a small surface area, the increasing of $TiO_2$ amount has less impact on the TCF photocatalytic activity in the dark adsorption.

Fig. 7b presents the photocatalytic reduction of Cr(VI) using TCF with different $TiO_2$ loading on the TCF as a function of time. The reaction followed a pseudo-first-order pattern and the plots of

Please cite this article in press as: Ananpattarachai, J., Kajitvichyanukul, P., Enhancement of chromium removal efficiency on adsorption and photocatalytic reduction using a bio-catalyst, titania-impregnated chitosan/xylan hybrid film, Journal of Cleaner Production (2015), http://dx.doi.org/10.1016/j.jclepro.2015.10.098

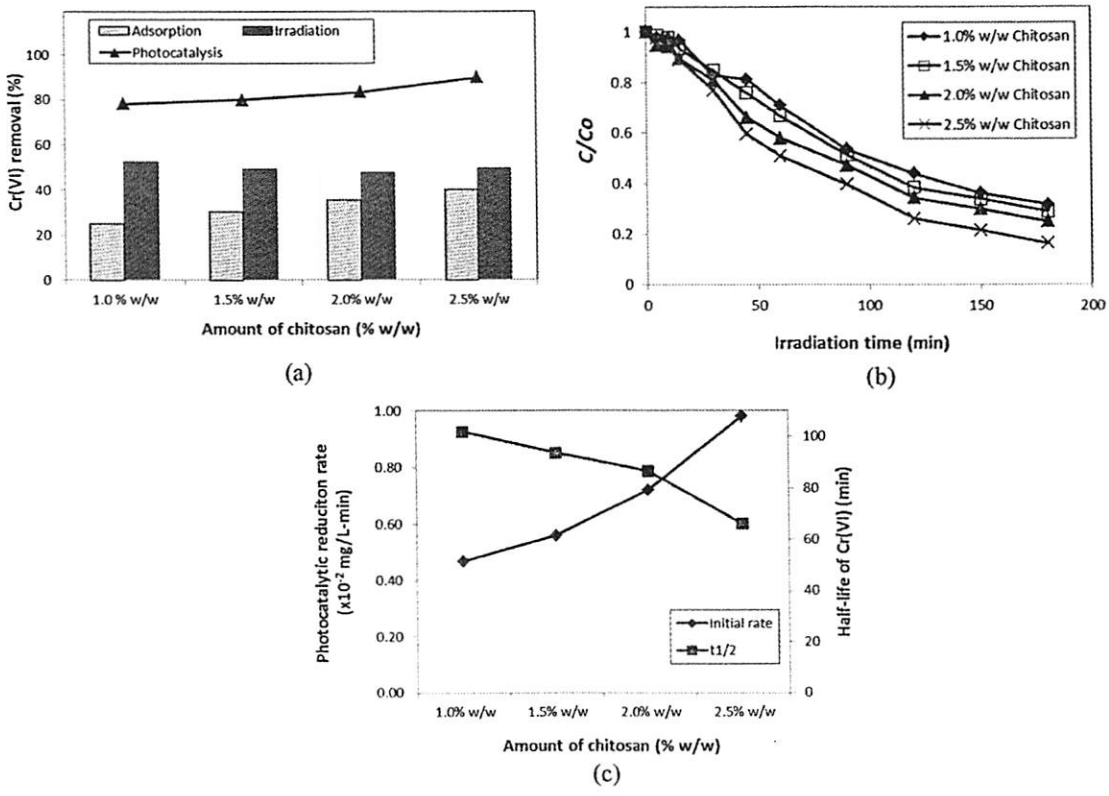


**Fig. 6.** Photocatalytic reduction of Cr(VI) with varying chitosan loadings: (a) Cr(VI) removal percentage versus chitosan loading, (b) residual fraction of Cr(VI) with time, (c) reaction rate and half-life of Cr(VI) versus chitosan loading. Conditions: TCF with 0.4% w/w $TiO_2$ and 0.1% w/v xylan, [Cr] = 150 ppm, pH 3.

**Table 4**
Values of kinetic parameters for photocatalytic reduction of Cr(VI) using TCF with varying chitosan loadings.

| Chitosan | $r \times 10^{-2}$ (mg/L-min) | $k_{obs}$ ($min^{-1}$) | Cr(VI) removal (%) | $R^2$ | $t_{1/2}$ (min) |
|---|---|---|---|---|---|
| 1.0% w/w | 0.47 | 0.0068 | 78.09 | 0.9920 | 101.93 |
| 1.5% w/w | 0.56 | 0.0074 | 79.92 | 0.9986 | 93.66 |
| 2.0% w/w | 0.72 | 0.0080 | 83.31 | 0.9916 | 86.64 |
| 2.5% w/w | 0.98 | 0.0105 | 89.79 | 0.9939 | 66.01 |

calculated photocatalytic reduction rate of Cr(VI) and the half-life of Cr(VI) during irradiation process under the variation of amount of $TiO_2$ in TCF are shown in Fig. 7c.

Results show that within 180 min irradiation in the presence of TCF catalyst, the Cr(VI) removal efficiency was highest with the application of maximum $TiO_2$ loading which is 0.8% w/w $TiO_2$ on TCF material. With the increasing $TiO_2$ loading in TCF, the reaction rate increased and the half-life of Cr(VI) decreased. The half-life of Cr(VI) had time lessening from 135.91 min to 63.59 min as increasing amount of $TiO_2$ in TCF from 0.2% w/w $TiO_2$ to 0.8% w/w $TiO_2$. The increasing of $TiO_2$ in TCF exerts the positive influence on the kinetics of photocatalytic reduction of Cr(VI). The reaction rate of TCF with 0.8% w/w $TiO_2$ was almost twofold higher than that of the TCF with 0.2% w/w $TiO_2$. The rate constant of the TCF with 0.2% w/w $TiO_2$ was only $5.1 \times 10^{-3}$ $min^{-1}$, whereas the rate constant of the TCF with 0.8% w/w $TiO_2$ was $10.9 \times 10^{-3}$ $min^{-1}$. Results obtained from this experimental set illustrated that the amount of $TiO_2$ was directly impacted on the photoactivity and kinetics of Cr(VI) photocatalytic reduction. The higher content of $TiO_2$ in TCF is, the greater quantity of Cr(VI) can be removed from the water during the irradiation process. The kinetic parameters of this reaction using TCF under different amount of $TiO_2$ were presented in Table 5.

### 3.7. Effect of Cr(VI) concentration on photocatalytic activity and kinetics

Effect of initial Cr(VI) concentration on photocatalytic reduction was evaluated by varying the initial Cr(VI) concentration from 50 to 300 ppm at initial pH 3. The TCF in this experiment was prepared from 1.4% w/w chitosan and 0.2% w/w $TiO_2$. The percentages of Cr(VI) removal in each stage of photocatalysis and total percentage removal were shown in Fig. 8a. The adsorption plays a major role in Cr(VI) removal when the initial concentration of Cr(VI) is very low (50 ppm). Approximately 67% of Cr(VI) concentration was removed during dark adsorption and only 33% of Cr(VI) concentration was eliminated during irradiation. As the initial concentration of Cr(VI) approached 100 ppm, the less adsorption percentage of Cr(VI) on TCF surface was obtained and the Cr(VI) removal by photoreaction did increase. At this point, approximately 38 and 62% of Cr(VI) concentration was removed by adsorption and irradiation process, respectively. Beyond 100 ppm of initial Cr(VI) concentration, the Cr(VI) removal efficiency in both processes was continuously decreased. The overall photocatalytic activity was also decreased from 100% to nearly 42.3% with increasing the initial Cr(VI) concentration from 50 to 300 ppm after 180 min. The increasing of Cr(VI) concentration results in adsorption increasing of Cr(VI) ions onto TCF materials,

Please cite this article in press as: Ananpattarachai, J., Kajitvichyanukul, P., Enhancement of chromium removal efficiency on adsorption and photocatalytic reduction using a bio-catalyst, titania-impregnated chitosan/xylan hybrid film, Journal of Cleaner Production (2015), http://dx.doi.org/10.1016/j.jclepro.2015.10.098

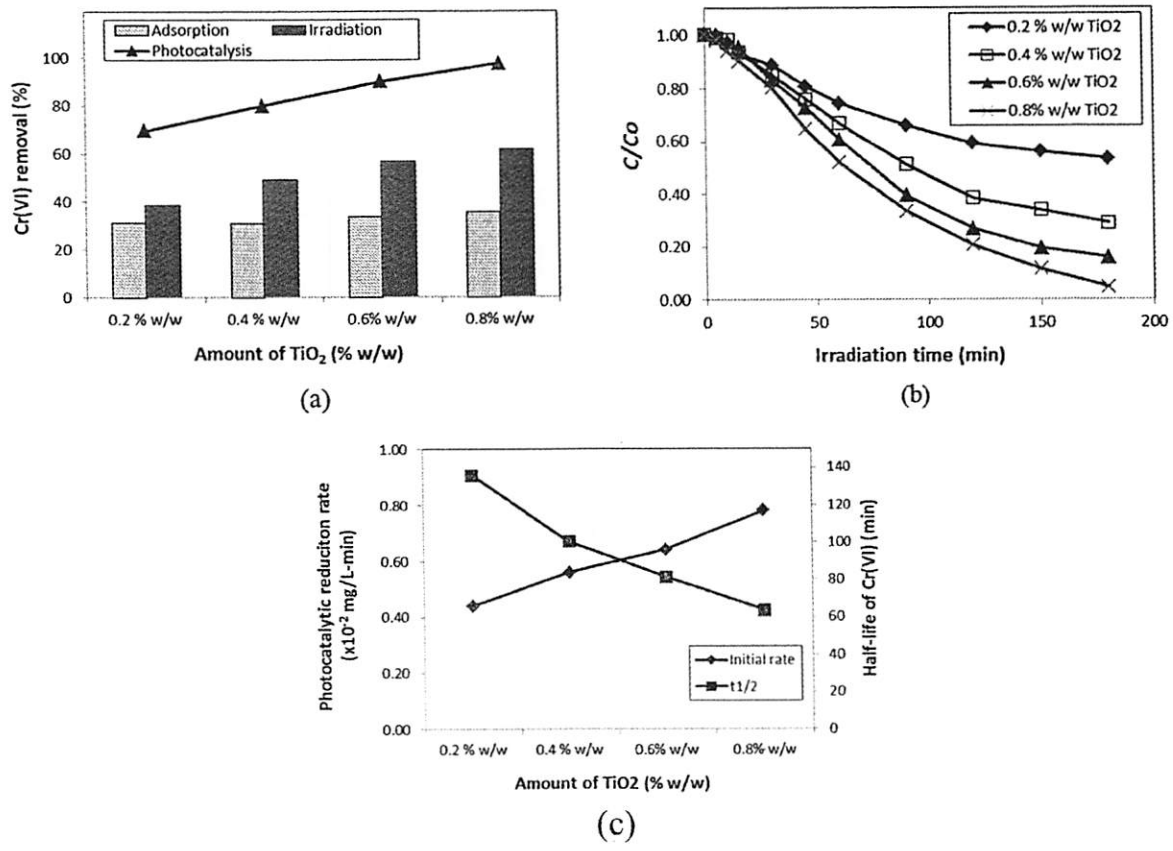


**Fig. 7.** Photocatalytic reduction of Cr(VI) with varying $TiO_2$ loadings: (a) Cr(VI) removal percentage versus $TiO_2$ loading, (b) residual fraction of Cr(VI) with time, (c) reaction rate and half-life of Cr(VI) versus $TiO_2$ loading. Conditions: TCF with 1.5% w/w chitosan and 0.1% w/v xylan, [Cr] = 150 ppm, pH 3.

**Table 5**
Values of kinetic parameters for photocatalytic reduction of Cr(VI) using TCF with varying $TiO_2$ loadings.

| $TiO_2$ | $r \times 10^{-2}$ (mg/L-min) | $k_{obs}$ ($min^{-1}$) | Cr(VI) removal (%) | $R^2$ | $t_{1/2}$ (min) |
|---|---|---|---|---|---|
| 0.2% w/w | 0.44 | 0.0051 | 69.63 | 0.9920 | 135.91 |
| 0.4% w/w | 0.56 | 0.0069 | 79.92 | 0.9986 | 100.45 |
| 0.6% w/w | 0.64 | 0.0085 | 90.01 | 0.9916 | 81.54 |
| 0.8% w/w | 0.78 | 0.0109 | 97.34 | 0.9939 | 63.59 |

which can cause inhibitive effect on further photocatalytic reduction of Cr(VI) because of the decreasing adsorption sites on the photocatalyst (Jiang et al., 2006). Similar results were also reported in previous work by other researcher (Naimi-Joubani et al., 2015).

Fig. 8b presents the photocatalytic reduction of Cr(VI) using TCF with different initial concentration of Cr(VI) as a function of time. Fig. 8c shows the plots of calculated photocatalytic reduction rate of Cr(VI) and the half-life of Cr(VI) during irradiation process. Results reveal that with increase in the concentration of Cr(VI), the photocatalytic reduction rate decreased. Decrease in photocatalytic reaction rate at higher concentration is attributed the fact that the equilibrium adsorption of Cr(VI) on the catalyst surface active site increases and more molecules of Cr(VI) get adsorbed on the surface of the catalyst. Therefore, the competitive adsorption of electron donor (such as $OH^-$) and electron acceptor (such as Cr(VI)) on the same site decreases and consequently the amount of radicals ($OH^\bullet$ and $O_2^{-\bullet}$) to complete the redox reaction in both photocatalytic oxidation and reduction reactions decreases. Consequently, the photocatalytic reaction rate becomes slower under higher concentration. In addition, the decreasing in the photocatalytic activity and the increasing of half-life of Cr(VI) are observed.

From Table 6, the increasing of initial concentration of Cr(VI) exerts the negative impact on the kinetics of photocatalytic reduction of Cr(VI) as the reaction rate was drastically reduce. The rate constant for 50 ppm initial concentration of Cr(VI) was $22.14 \times 10^{-2}$ $min^{-1}$, whereas the rate constant for 300 ppm initial concentration of Cr(VI) was $0.26 \times 10^{-2}$ $min^{-1}$. The results demonstrated that the initial concentration of Cr(VI) decreased the photoactivity and kinetics of Cr(VI) photocatalytic reduction.

### 3.8. Kinetic modelling

The photocatalytic reaction of model pollutants can be well described by the Langmuir–Hinshelwood (L–H) kinetic model. The rate of a unimolecular surface reaction, $R$, is proportional to the surface coverage, $\theta$, when the reactant is more strongly adsorbed on the surface than the products. The Langmuir–Hinshelwood rate expression was applied for heterogeneous photocatalytic reduction using TCF to determine the relationship between the initial reaction rate and the initial concentration of Cr(VI). The L–H model express as:

Please cite this article in press as: Ananpattarachai, J., Kajitvichyanukul, P., Enhancement of chromium removal efficiency on adsorption and photocatalytic reduction using a bio-catalyst, titania-impregnated chitosan/xylan hybrid film, Journal of Cleaner Production (2015), http://dx.doi.org/10.1016/j.jclepro.2015.10.098

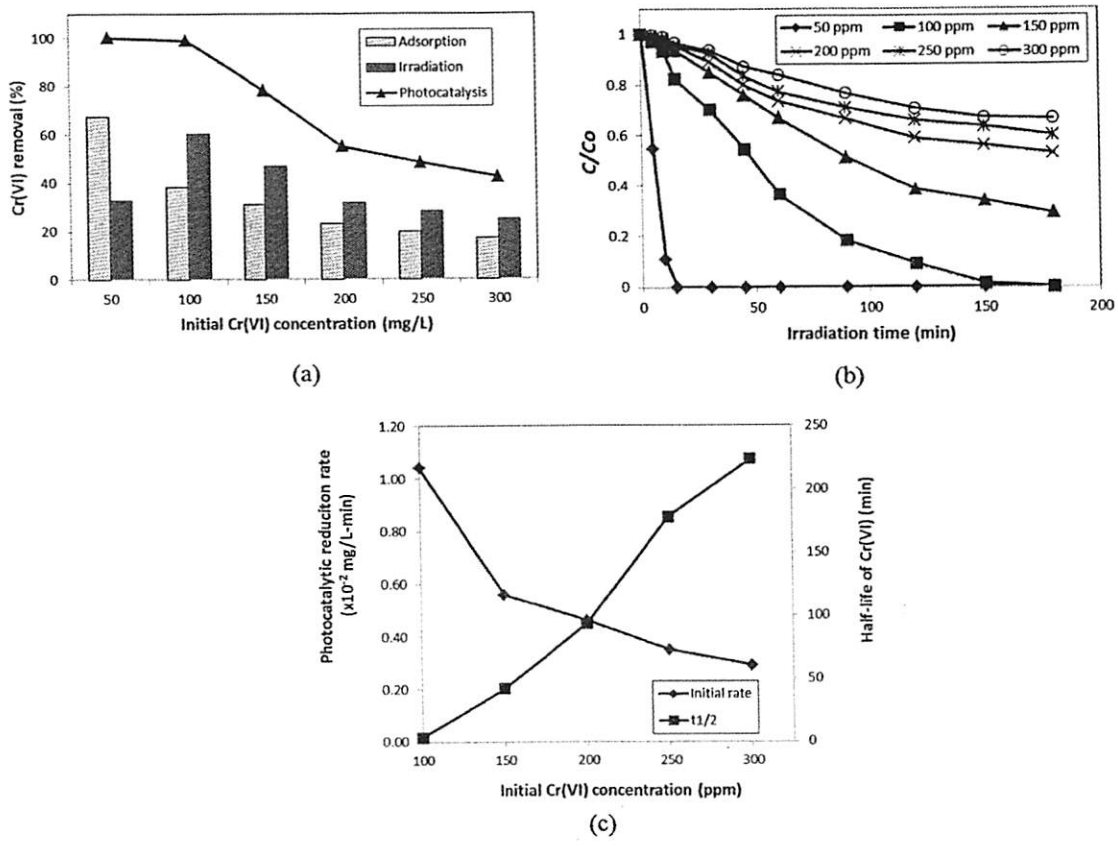


**Fig. 8.** Photocatalytic reduction of Cr(VI) with varying Cr(VI) concentrations: (a) Cr(VI) removal percentage versus Cr(VI) concentration, (b) residual fraction of Cr(VI) with time, (c) reaction rate and half-life of Cr(VI) versus Cr(VI) concentration. Conditions: TCF with 1.5% w/w chitosan, 0.4 $TiO_2$, and 0.1% w/w xylan, [Cr] = 50–300 ppm, pH 3.

**Table 6**
Values of kinetic parameters for photocatalytic reduction of Cr(VI) using TCF with varying Cr(VI) concentrations.

| $TiO_2$ | $r \times 10^{-2}$ (mg/L-min) | $k_{obs}$ ($min^{-1}$) | Cr(VI) removal (%) | $R^2$ | $t_{1/2}$ (min) |
|---|---|---|---|---|---|
| 50 ppm | 6.87 | 0.2214 | 100.00 | 0.936 | 3.13 |
| 100 ppm | 1.04 | 0.0164 | 100.00 | 0.9726 | 42.27 |
| 150 ppm | 0.56 | 0.0074 | 79.92 | 0.9915 | 93.67 |
| 200 ppm | 0.46 | 0.0039 | 60.74 | 0.9702 | 177.73 |
| 250 ppm | 0.35 | 0.0031 | 53.05 | 0.9648 | 223.60 |
| 300 ppm | 0.29 | 0.0026 | 46.3 | 0.9725 | 266.60 |

$$R = -dC/dt = k_r\theta = (k_r \cdot K_{LH} \cdot C_0)/(1 + K_{LH} \cdot C_0 + K_S \cdot C_S) \quad (7)$$

$$R = -dC/dt = k_r\theta = (k_r \cdot K_{LH} \cdot C_0)/(1 + K_{LH} \cdot C_0 R) \quad (8)$$

where $k_r$ is the rate constant of surface reaction, $\theta$ is fraction of the surface covered by the reactant, $K_{LH}$ is the Langmuir–Hinshelwood adsorption equilibrium constant, $C_0$ is initial concentration of the reactant, $K_S$ is adsorption coefficient of the solvent, and $C_S$ is concentration of the solvent.

**Table 7**
Values of Langmuir–Hinshelwood kinetic parameters for photocatalytic reduction of Cr(VI) using seven types of TCF.

| $TiO_2$ | Chitosan | Xylan | $k_r$ | $K_{LH}$ (mg/L-min) | $R^2$ (L/mg) |
|---|---|---|---|---|---|
| 0.2% w/w | 1.5% w/w | 0.1% w/w | 0.4091 | 0.0236 | 0.9779 |
| 0.4% w/w | 1.5% w/w | 0.1% w/w | 0.6234 | 0.0581 | 0.9876 |
| 0.6% w/w | 1.5% w/w | 0.1% w/w | 0.6463 | 0.0392 | 0.9912 |
| 0.8% w/w | 1.5% w/w | 0.1% w/w | 0.7319 | 0.0387 | 0.9908 |
| 0.4% w/w | 1.0% w/w | 0.1% w/w | 0.5413 | 0.0494 | 0.9874 |
| 0.4% w/w | 2.0% w/w | 0.1% w/w | 0.6522 | 0.0435 | 0.9934 |
| 0.4% w/w | 2.5% w/w | 0.1% w/w | 0.7211 | 0.0451 | 0.9986 |

In this work, concentrations of Cr(VI) ranging between 50 and 300 ppm were conducted at the optimal conditions of pH 3 under illumination of ultraviolet light. Seven types of TCF were investigated. The L–H kinetic model was applied to the photocatalytic reduction of Cr(VI) which was successfully fitted and can be described by the pseudo-first order kinetic, as confirmed by the obtained straight line. The values of $k_r$, $K_{LH}$, and $R^2$ are shown in Table 7. According to the L–H model, the photocatalytic rate constant ($k_r$) of surface reaction of Cr(VI) was increased with an increase of the amount of $TiO_2$ and chitosan in TCF catalyst because of the additional available active sites ($\theta$) for adsorption. The Langmuir–Hinshelwood adsorption equilibrium constant ($K_{LH}$) was increased with increasing of the amount of $TiO_2$ and chitosan in TCF catalyst to a certain value before decreasing at high chemical loading (either chitosan or $TiO_2$). This behaviour can be explained by the fact that the high chitosan loading on TCF introduced the dense film of chitosan/xylan hybrid material (as shown in SEM

Please cite this article in press as: Ananpattarachai, J., Kajitvichyanukul, P., Enhancement of chromium removal efficiency on adsorption and photocatalytic reduction using a bio-catalyst, titania-impregnated chitosan/xylan hybrid film, Journal of Cleaner Production (2015), http://dx.doi.org/10.1016/j.jclepro.2015.10.098

image, Fig. 3c) that shielded the nano$TiO_2$ powder. In addition, high $TiO_2$ loading can cause the agglomeration of nanoparticles on the TCF surface. These changes on surface morphology may reduce the equilibrium adsorption ability of TCF and reflect on the $K_{LH}$ value. The highest $K_{LH}$, 5.81 × $10^{-2}$ L/mg, was obtained with the application of TCF with 0.4% w/w $TiO_2$ and 1.5% w/w chitosan.

## 4. Conclusion

A $TiO_2$-impregnated chitosan/xylan hybrid film (TCF) was synthesized and applied as a bio-catalyst to remove Cr(VI) in water by adsorption and photocatalysis process. The novel sorbent TCF is capable of Cr(VI) removal and it was successfully shown to be competitive with chitosan film and $TiO_2$ powder. The protonated amino group ($-NH_3^+$) which was a functional of the chitosan biopolymer plays role in enhancing the adsorption of Cr(VI) onto TCF surface. pH has a substantial effect on performance of TCF in Cr(VI) adsorption. The optimum pH in Cr(VI) removal by TCF was found at pH 3.

Adsorption isotherm pattern of $TiO_2$/chitosan bio-catalyst for Cr(IV) removal followed the Langmuir adsorption isotherm model. Pseudo-first order pattern well described the photocatalytic reduction reactions of Cr(VI) using TCF catalyst. The photocatalytic performance can be enhanced by the impregnation of $TiO_2$ into chitosan/xylan hybrid matrix. TCF catalyst can remove Cr(VI) from aqueous solution with a higher efficiency than $TiO_2$ powder. The photocatalytic reduction rate of Cr(VI) was 0.56 × $10^{-3}$ and 0.03 × $10^{-3}$ ppm-min for TCF and $TiO_2$ powder, respectively. The increasing of chitosan amount in TCF enhanced the adsorption ability of the TCF and the kinetics of photocatalytic reaction. The rate constant of the TCF with 1.0% w/w chitosan was only 6.8 × $10^{-3}$ $min^{-1}$, whereas the rate constant of the TCF with 2.5% w/w chitosan was 10.5 × $10^{-3}$ $min^{-1}$. The reaction rate of TCF with 2.5% w/w chitosan was twofold higher than that of the TCF with 1.0% w/w chitosan. The $TiO_2$ loading in TCF was directly impact on the photoactivity and kinetics of Cr(VI) photocatalytic reduction. The higher content of $TiO_2$ in TCF, the higher quantity of Cr(VI) can be removed from the water during irradiation process. With the increasing $TiO_2$ loading in TCF, the reaction rate increased and the half-life of Cr(VI) decreased. The half-life of Cr(VI) had time lessening from 135.91 min to 63.59 min as increasing amount of $TiO_2$ in TCF from 0.2% w/w $TiO_2$ to 0.8% w/w $TiO_2$. Results from this work reveal that TCF exhibited high efficiency in photocatalytic activity.

In the application of $TiO_2$ in water/wastewater treatment, the neat $TiO_2$ nanopowder required filtration unit after removal of heavy metals from the waste stream, whereas TCF was taken off from the reactor to separate treated water from the bio-catalyst. This simple mode of separation can be benefit for industry scale up to a commercial level. This synthesized TCF has a high potential to be used as a catalyst for photocatalysis process in industrial scale to remove heavy metals from the waste stream.

## Acknowledgement

This research was supported by Naresuan University Research (No. R2558B024) through Center of Excellence on Environmental Research and Innovation, Faculty of Engineering, Naresuan University.

## References

Abou El-Reash, Y.G., Otto, M., Kenawy, I.M., Ouf, A.M., 2011. Adsorption of Cr(VI) and As(V) ions by modified magnetic chitosan chelating resin. Int. J. Biol. Macromol. 49, 513–522. http://dx.doi.org/10.1016/j.ijbiomac.2011.06.001.

Bhaumik, M., Maity, A., Srinivasu, V.V., Onyango, M.S., 2011. Enhanced removal of Cr(VI) from aqueous solution using polypyrrole/$Fe_3O_4$ magnetic nanocomposite. J. Hazard. Mater. 190, 381–390. http://dx.doi.org/10.1016/j.jhazmat.2011.03.062.

Cara, P.D., Pagliaro, M., Elmekawy, A., Brown, D.R., Verschuren, P., Shiju, N.R., Rothenberg, G., 2013. Hemicellulose hydrolysis catalysed by solid acids. Catal. Sci. Technol. 3, 2057–2061. http://dx.doi.org/10.1039/C3CY20838A.

Cheung, W.H., Szeto, Y.S., McKay, G., 2009. Enhancing the adsorption capacities of acid dyes by chitosan nano particles. Bioresour. Technol. 100, 1143–1148. http://dx.doi.org/10.1016/j.biortech.2008.07.071.

Chong, M.N., Cho, Y.J., Poha, P.E., Jin, B., 2015. Evaluation of Titanium dioxide photocatalytic technology for the treatment of reactive Black 5 dye in synthetic and real greywater effluents. J. Clean. Prod. 89, 196–202. http://dx.doi.org/10.1016/j.jclepro.2014.11.014.

Crini, G., Badot, P.M., 2008. Application of chitosan, a natural aminopolysaccharide, for dye removal from aqueous solutions by adsorption processes using batch studies: a review of recent literature. Prog. Polym. Sci. 33, 399–447. http://dx.doi.org/10.1016/j.progpolymsci.2007.11.001.

Dai, B.Y., Cao, M.R., Fang, G.Z., Liu, B., Dong, X., Pan, M.F., Wang, S., 2012. Schiff base-chitosan grafted multiwalled carbon nanotubes as a novel solid-phase extraction adsorbent for determination of heavy metal by ICP-MS. J. Hazard. Mater. 219–220, 103–110. http://dx.doi.org/10.1016/j.jhazmat.2012.03.065.

Dodd, D., Mackie, R.I., Cann, I.K.O., 2011. Xylan degradation, a metabolic property shared by rumen and human colonic bacteroidetes. Mol. Microbiol. 79, 292–304. http://dx.doi.org/10.1111/j.1365-2958.2010.07473x.

Doke, K.M., Khan, E.M., 2012. Equilibrium, kinetic and diffusion mechanism of Cr(VI) adsorption onto activated carbon derived from wood apple shell. Arab. J. Chem. http://dx.doi.org/10.1016/j.arabjc.2012.07.031 (in press).

Eastmond, D.A., MacGregor, J.T., Slesinski, R.S., 2008. Trivalent chromium: assessing the genotoxic risk of an essential trace element and widely used human and animal nutritional supplement. Crit. Rev. Toxicol. 38, 173–190.

Gerente, C., Lee, V.K.C., Le Cloirec, P., McKay, G., 2007. Application of chitosan for the removal of metals from wastewaters by adsorption – mechanisms and models review. Crit. Rev. Environ. Sci. Technol. 37, 41–127. http://dx.doi.org/10.1080/10643380600729089.

Huang, G.L., Zhang, H.Y., Shi, J.X., Langrish, T.A.G., 2009. Adsorption of chromium(VI) from aqueous solutions using cross-linked magnetic chitosan beads. Ind. Eng. Chem. Res. 48, 2646–2651. http://dx.doi.org/10.1021/ie800814h.

Jiang, F., Zheng, Z., Xu, Z., Zheng, S., Guo, Z., Chen, L., 2006. Aqueous Cr(VI) photoreduction catalyzed by $TiO_2$ and sulfated $TiO_2$. J. Hazard. Mater. 134, 94–103. http://dx.doi.org/10.1016/j.jhazmat.2005.10.041.

Kajitvichyanukul, P., Amornchat, P., 2005. Effects of diethylene glycol on $TiO_2$ thin film properties prepared by sol-gel process. Sci. Technol. Adv. Mater. 6, 344–347.

Kajitvichyanukul, P., Watcharenwong, A., 2003. Role of pH, organic and inorganic anions on photocatalytic reduction of chromium (VI) with titania powders. Asian J. Sci. Technol. Dev. 22, 169–179.

Kajitvichyanukul, P., Ananpattarachai, J., Pongpom, S., 2005. Sol-gel preparation and properties study of $TiO_2$ thin film for photocatalytic reduction of chromium(VI) in photocatalysis process. Sci. Technol. Adv. Mater. 6, 352–358. http://dx.doi.org/10.1016/j.stam.2005.02.014.

Leceta, I., Guerrero, P., Cabezudo, S., de la Cab, K., 2013. Environmental assessment of chitosan-based films. J. Clean. Prod. 41, 312–318. http://dx.doi.org/10.1016/j.jclepro.2012.09.049.

Makeswari, M., Santhi, T., 2014. Adsorption of Cr(VI) from aqueous solutions by using activated carbons prepared from Ricinus communis leaves: binary and ternary systems. Arab. J. Chem. http://dx.doi.org/10.1016/j.arabjc.2013.10.005 (in press).

Naimi-Joubani, M., Shirzad-Siboni, M., Yang, J.-K., Gholami, M., Farzadki, M., 2015. Photocatalytic reduction of hexavalent chromium with illuminated ZnO/$TiO_2$ composite. J. Ind. Eng. Chem. 22, 317–323. http://dx.doi.org/10.1016/j.jiec.2014.07.025.

Nawi, M.A., Jawad, Ali H., Sabar, S., Wan Ngah, W.S., 2011. Immobilized bilayer $TiO_2$/chitosan system for the removal of phenol under irradiation by a 45 watt compact fluorescent lamp. Desalination 280, 288–296. http://dx.doi.org/10.1016/j.desal.2011.07.013.

Said, Z., Sabiha, M.A., Saidura, R., Hepbasli, A., Rahim, N.A., Mekhilef, S., Ward, T.A., 2015. Performance enhancement of a flat plate solar collector using Titanium dioxide nanofluid and polyethylene glycol dispersant. J. Clean. Prod. 92, 343–353. http://dx.doi.org/10.1016/j.jclepro.2015.01.007.

Sankararamakrishnan, N., Dixit, A., Iyengar, L., Sanghi, R., 2005. Removal of hexavalent chromium using a novel cross linked xanthated chitosan. Bioresour. Technol. 50, 850–858. http://dx.doi.org/10.1016/j.biortech.2005.10.024.

Wu, S., Hu, J., Wei, L., Du, Y., Shi, X., Deng, H., Zhang, L., 2014. Construction of porous chitosan–xylan–$TiO_2$ hybrid with highly efficient sorption capability on heavy metals. J. Environ. Chem. Eng. 2, 1568–1577. http://dx.doi.org/10.1016/j.jece.2014.07.001.

Zhou, X., Korenaga, T., Takahashi, T., Moriwake, T., Shinoda, S., 1993. A process monitoring/controlling system for the treatment of wastewater containing chromium(VI). Water Res. 27, 1049–1054. http://dx.doi.org/10.1016/0043-1354(93)90069-T.

Please cite this article in press as: Ananpattarachai, J., Kajitvichyanukul, P., Enhancement of chromium removal efficiency on adsorption and photocatalytic reduction using a bio-catalyst, titania-impregnated chitosan/xylan hybrid film, Journal of Cleaner Production (2015), http://dx.doi.org/10.1016/j.jclepro.2015.10.098